Whole body adhesion: hierarchical, directional and distributed control of adhesive forces for a climbing robot

Sangbae Kim, Matthew Spenko, Salomon Trujillo, Barrett Heyneman, Virgilio Mattoli, Mark R. Cutkosky
Center for Design Research
Stanford University
Stanford, CA 94305-2232, USA
contact: sangbae@stanford.edu

***Abstract*— We describe the design and control of a new bio-inspired climbing robot designed to scale smooth vertical surfaces using directional adhesive materials. The robot, called Stickybot, draws its inspiration from geckos and other climbing lizards and employs similar compliance and force control strategies to climb smooth vertical surfaces including glass, tile and plastic panels. Foremost among the design features are multiple levels of compliance, at length scales ranging from centimeters to micrometers, to allow the robot to conform to surfaces and maintain large real areas of contact so that adhesive forces can support it. Structures within the feet ensure even stress distributions over each toe and facilitate engagement and disengagement of the adhesive materials. A force control strategy works in conjunction with the directional adhesive materials to obtain sufficient levels of friction and adhesion for climbing with low attachment and detachment forces.**

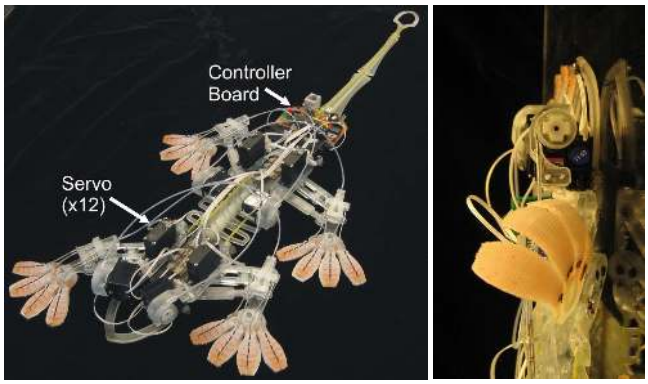

Fig. 1. Left: Stickybot, a new bio-inspired robot capable of climbing smooth surfaces. Right: a sideview of Stickybot climbing vertical glass.

I. Introduction

Robots capable of climbing vertical surfaces would be useful for disaster relief, surveillance, and maintenance applications. Various robots have used suction [15], [29] and magnets [5], [26] for climbing smooth surfaces. A controlled vortex that creates negative aerodynamic lift has also been demonstrated [24]; however, it requires substantial power and generates noise even when stationary. Microspines, drawing inspiration from insects and spiders, have been used to climb rough surfaces such as brick and concrete [1], [19].

For climbing on a range of vertical surfaces from smooth glass to rough stucco, various animals including insects, spiders, tree frogs and geckos employ wet or dry adhesion. The impressive climbing performance of these creatures has lead to a number of robots that employ adhesives for climbing. Sticky adhesives have the disadvantage that they quickly become dirty and lose adhesion [9], [22]. Another disadvantage is that the adhesive requires relatively high forces for attachment and detachment, although researchers have mitigated this problem by using clever spoked-wheel designs that allow the detachment forces at a receding point of contact to provide the necessary attachment force at the next contact.

To overcome the issue of fouling, there has been a trend toward developing "dry adhesives" which generally have a higher elastic modulus than PSAs and rely on van der Waals forces between arrays of microscopic features and the substrate for adhesion. These have been modeled on the adhesive properties of geckos [4]. In other work, climbing robots have used elastomeric microstructured tape or elastomeric pads that attract dirt after repeated use but, in contrast to PSAs, can be cleaned with water and reused [8], [23], [11], [14], [18]. As feature sizes grow smaller, increasingly stiff and hydrophobic materials can be used while still obtaining sufficient real areas of contact for van der Waals forces to provide useful levels of adhesion [10], [17]. The result is an adhesive that resists dirt accumulation. Various groups are working on synthetic dry adhesives [16], [20], [28]. Currently, no single solution generates high adhesion, attaches with low preload, and is rugged and self-cleaning; however, there is steady progress in each of these directions.

This paper argues that three interconnected design principles are essential for a legged robot to climb and maneuver on vertical surfaces using dry adhesion:

1) hierarchical compliance for conforming at centimeter, millimeter, and micrometer scales;
2) directional adhesives so that the robot can control adhesion by controlling shear; and
3) distributed force control that works with compliance and anisotropy to achieve stability.

This paper reviews these principles in the gecko and describes how they are implemented on Stickybot, a new bio-inspired quadruped robot designed to climb smooth vertical surfaces (Fig. 1). Experimental results of Stickybot climbing glass are included. The paper concludes with discussion of ongoing work to improve the reliability and performance of Stickybot. A companion paper [18] describes the detailed

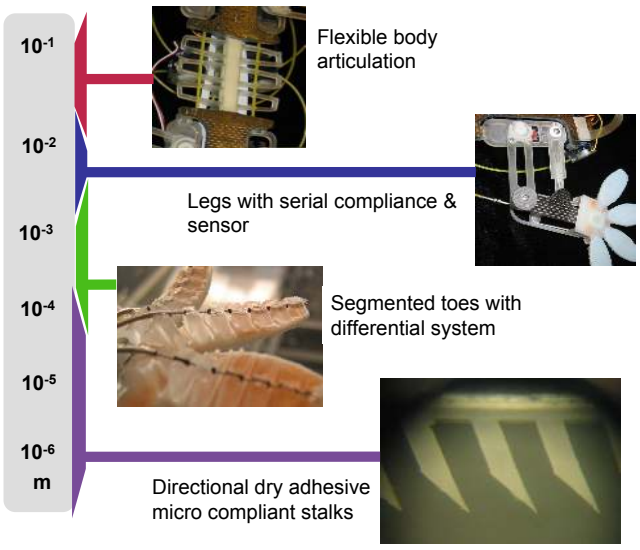

Fig. 2. Illustration of Stickybot's hierarchical compliance over a range of length scales.

design, fabrication and performance of the adhesive patches.

II. Design Principles for Climbing with Dry Adhesion

This section describes how the principles of hierarchical compliance, directional adhesion, and distributed force control are applied to Stickybot.

A. Hierarchical Compliance

Climbing with van der Waals forces requires intimate contact because the forces scale as A/d^3 where A is the Hammacher constant and d is the local separation between two surfaces. For particular material combinations the Hammacher constant can vary by as much as a factor of 4 [27]. However, reducing the separation distance has a much greater effect, making it essential to comply to natural and artificial surfaces, which commonly have an approximately fractal surface topography.

In the gecko, the flex of the body and limbs allows for conformation at the centimeter scale. The feet are divided into several toes that can conform independently at a scale of several millimeters. The bottom surfaces of toes are covered with lamellae that conform at the millimeter scale. The lamellae are composed of many individual setae, each of which acts as a spring-loaded beam that provides conformability at the 1-50 micrometer scale. The tips of the setae are divided into hundreds of spatulae that provide conformability at the $<$500 nanometer scale. The consequence of the gecko's hierarchical system of compliances is that it can achieve levels of adhesion of over 500 KPa on a wide variety of surfaces from glass to rough rock and can support its entire weight from just one toe [4].

To enable Stickybot to climb a variety of surfaces an analogous, albeit much less sophisticated, hierarchy of compliances has been employed (Fig. 2). The body of Stickybot is a highly compliant under-actuated system comprised of 12 servos and 38 degrees of freedom. The torso and limbs are created via Shape Deposition Manufacturing [25], [6] using two different grades of polyurethane (Innovative Polymers: 72 Shore-DC and 20 Shore-A hardness).

The stiffest and strongest components of Stickybot are the upper and lower torso and the forelimbs, which are reinforced with carbon fiber. The central part of the body represents a compromise between sufficient compliance to conform to gently curved surfaces and sufficient stiffness so that maximum normal forces of approximately +/- 1N can be applied at the feet without producing excessive body torsion. Additionally, the spine structure at the center of body has the ability to provide body articulation for greater maneuverability in the future.

Each limb is equipped with four segmented toes comprised of two grades of polyurethane and reinforced with embedded synthetic cloth fiber (Fig. 3). A single servomotor actuates the toes using a double-rocker linkage and steel cables in metal sleeves (Fig. 4) that allow the toes to attach independently to objects with a minimum radius of curvature of 5cm. The toes can also peel backward in a motion approximating the digital hyperextension that geckos use to detach their feet with very little force.

Assuming an approximately uniform toe width, the toe's cable profile is calculated to achieve a uniform stress distribution when the toes are deployed on flat surfaces (Fig. 5). The sum of the forces in the y direction is given as:

$$T\sin\theta - T\sin\left(\theta+\delta\theta\right) + F_n = 0 \tag{1}$$

where T is the force acting along the cable, θ is the angle of the cable with respect to the horizontal, and F_n is the normal force acting on the bottom of the toe. To ensure uniform attachment of the foot, a constant pressure on the bottom of the toe is desired:

$$\frac{T\left(\sin\left(\theta+d\theta\right)-\sin\theta\right)}{dx} = \frac{F_n}{dx} = \sigma \tag{2}$$

Expanding the term $\sin\left(\theta+d\theta\right)$ and assuming that $d\theta$ is

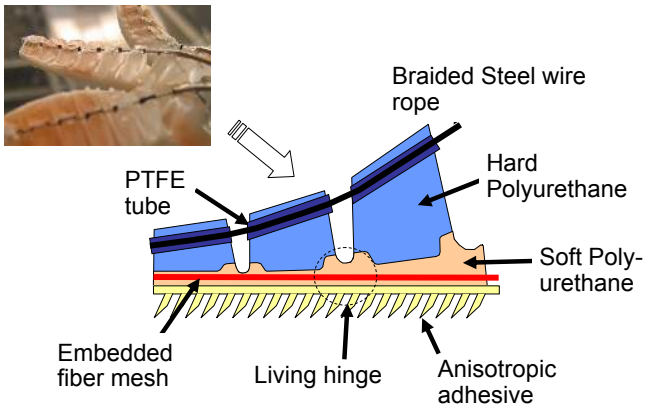

Fig. 3. Schematic of cross section view of Stickybot toe fabricated via Shape Deposition Manufacturing.

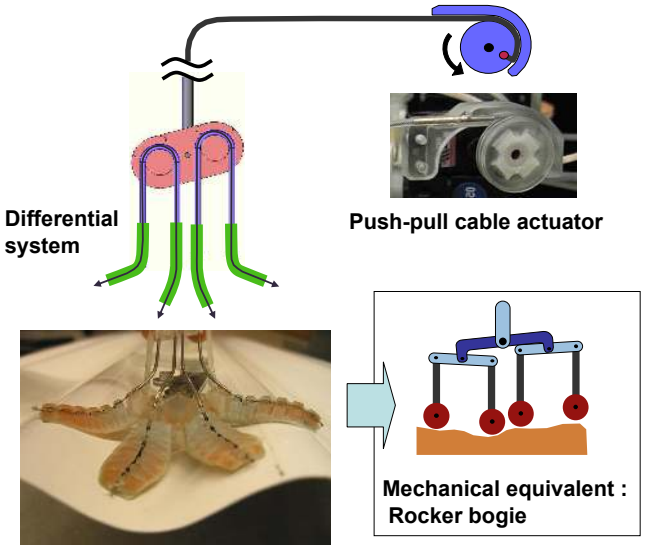

Fig. 4. The two stage differential system actuated by a single push pull actuator facilitates conformation on uneven surfaces and distributes the contact forces among four toes.

small such that $\cos d\theta = 1$ and $\sin d\theta = d\theta$ yields:

$$\cos\theta d\theta = \frac{\sigma}{T} dx \tag{3}$$

Integrating both sides and solving for θ gives the slope of the cable profile:

$$\frac{dy}{dx} = \tan\left(\arcsin\left(\frac{\sigma x}{T}\right)\right) \tag{4}$$

Integrating with respect to x yields the profile of the cable:

$$y\left(x\right) = -\frac{T}{\sigma}\sqrt{1-\left(\frac{\sigma x}{T}\right)^2} \tag{5}$$

which is simply a circular arc with radius T/σ.

At the finest scale, the contact surfaces of the feet are equipped with synthetic adhesive materials (Fig. 3). To date, the best results have been obtained with arrays of small, asymmetric elastomeric features as shown in Fig. 6. The arrays are made by micromolding with a soft (Shore 20-A) urethane polymer [18]. This structure allows anisotropic compliance that is essential for the directional adhesive behavior addressed in following section. Continued research involves alternative methods of fabrication with stiffer materials and smaller feature sizes to allow for additional levels of hierarchy.

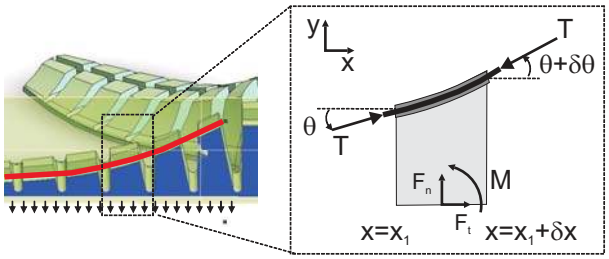

Fig. 5. Details of nomenclature used to calculate cable profile of the toes.

B. Directional Adhesion

As mentioned in the previous section, geckos can achieve adhesion greater than 500 KPa over areas of several square millimeters. However, adhesion only occurs if the lamellae and setae are loaded in the proper direction (inward from the distal toward the proximal region of the toes) [2]. The maximum pull-off force is related directly to the amount of tangential force present. Conversely, if the toes are brought into contact while moving from the proximal toward the tip regions (i.e., pushing along the toes rather than pulling) no adhesion is observed and the tangential force is limited by a coefficient of friction. The tangential and normal force limits can be modeled as:

$$\begin{array}{c} F_N \geq -\frac{1}{\mu} F_T \\ F_N \geq -\tan\left(\alpha*\right) F_T \end{array} \quad \begin{cases} F_T < 0 \\ 0 \leq F_T \leq F_{\max} \end{cases} \tag{6}$$

where $\alpha*$ is the critical peel angle [2], μ is the coefficient of friction, F_T is tangential (shear) load, taken positive when pulling inward, and F_N is the normal force, taken positive when compressive. The limit, F_{max}, is a function of the maximum tangential load that the gecko or robot can apply, the material strength, and the shear strength of the contact interface. Thus, adhesion increases proportionally with tangential force. This feature, coupled with the gecko's hierarchical compliance, allows it to adhere to surfaces without applying a significant preload, which can cause a gecko (or robot) to push itself away from the wall. Additionally, by decreasing the tangential load, the gecko is able to release its foot from the wall with negligible detachment force. Figure 7 illustrates the directional adhesion model in comparison to the commonly used isotropic Johnson-Kendall-Roberts (JKR) model for elastomers [13]. In contrast to the frictional adhesion model, the JKR model's limit surface does not intersect the origin. Instead, the maximum adhesion force is obtained when there is zero tangential force, which is much less useful for climbing vertical surfaces. Moreover, detachment requires a high normal force unless a high tangential force is also present.

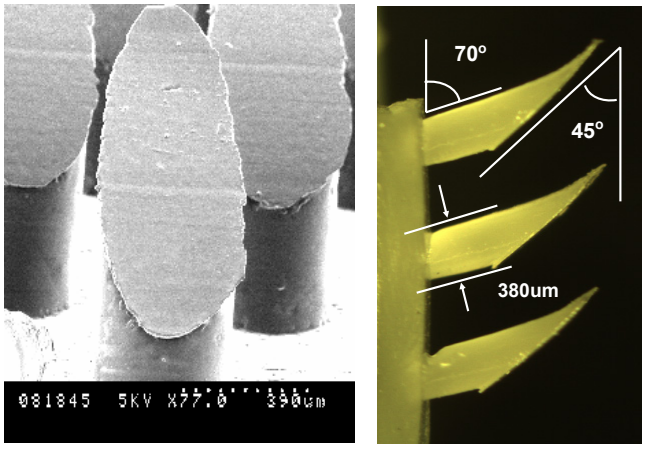

Fig. 6. Directional stalks comprised of 20 Shore-A polyurethane. Hairs measure 380 μm in diameter at the base. The base angle is 20° and the tip angle is 45°.

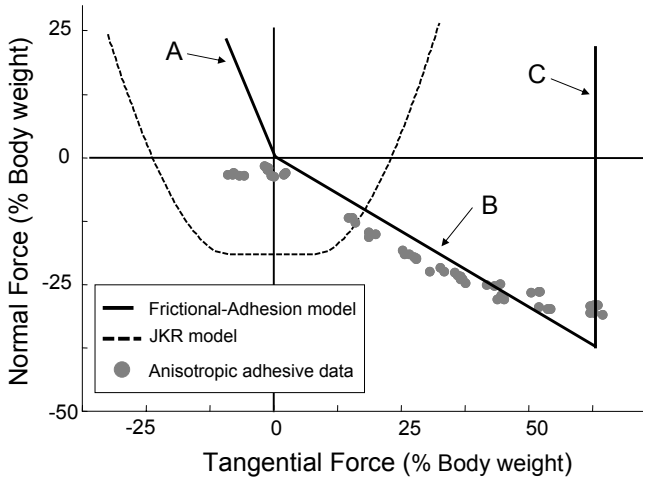

Fig. 7. Comparison of the frictional-adhesion model [2] and the Johnson-Kendall-Roberts (JKR) model [13] with pull off force data from a single toe of Stickybot's directional patches (513 stalks). (A) When dragged against the preferred direction, the directional patch exhibits negligible adhesion, although it sustains greater tangential force than expected from Coulomb friction when the normal force is zero. (B) When dragged in the preferred direction, the directional patch demonstrates adhesion proportional to the shear force, albeit with saturation at the highest levels. (C) The frictional-adhesion model has an upper shear force limit. In comparison, the JKR model shows typical behavior of an isotropic elastic material with adhesion.

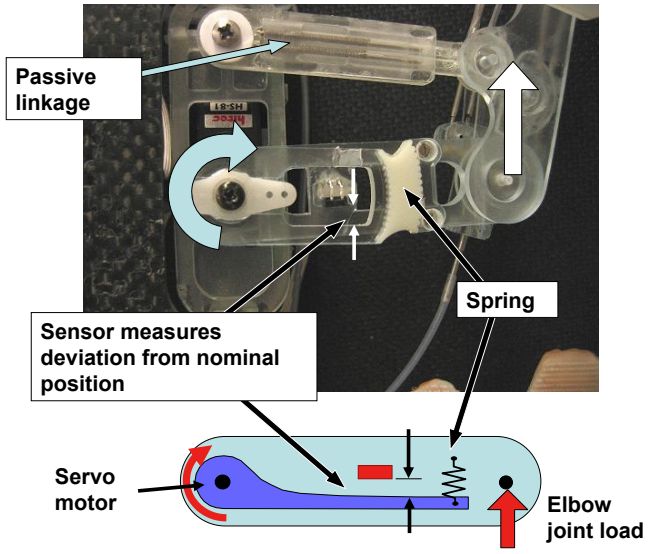

Fig. 8. Traction force sensor measuring deviation of serial compliance at shoulder joint.

Stickybot's directional adhesive patches approximately follow the frictional-adhesion model [2] as shown in Fig. 7. Evidence of low preload and detachment forces is presented in the Results section. Details of the design and performance of the patches are provided in [18]. Early versions of Stickybot used flat adhesive patches comprised of polyurethane (Innovative Polymers Shore 20A) or Sorbothane®. The large detachment forces caused undesirable force transients to propagate throughout the body and prematurely detach the other feet. Reliable climbing was not obtained until the anisotropic features were added.

C. Distributed Force Control

Distributed force control ensures that stresses are uniformly distributed over the toes and that undesirable force transients and accompanying oscillations are avoided. At the toe level, embedded flexible fabric (Fig. 3) allows the feet to obtain a more uniform shear loading over the toes. Together, the fabric and the cable "tendons" provide a load path that routes tangential forces from the toes to the ankles without producing undesired bending moments or stretching that would cause crack propagation and premature peeling at one edge of a toe. At the foot level, ankle compliance and a two stage differential mechanism balance normal forces among toes. At the body level, Stickybot utilizes force control to manage the tangential forces at the feet. This allows Stickybot to maintain dynamic equilibrium as well as increase or decrease the allowable adhesion force (as dictated by the frictional-adhesion model). In Stickybot, as in geckos, the combination of toe peeling (digital hyperextension) and directional adhesion are used to minimize detachment forces. To achieve smooth engagement and disengagement and control its internal forces, Stickybot uses force feedback coupled with a stiffness controller. Stickybot has force sensors located on its shoulder joints (Fig. 8) that measure the deflection of an elastomeric spring via a ratiometric Hall effect sensor (Honeywell: SS495A). In addition to providing an estimate of the force, the compliance helps to distribute forces among the limbs such that excessive internal forces do not occur and lead to contact failure.

Stickybot is controlled using a single master microcontroller (PIC18F4520) connected to four slave microcontrollers (PIC12F683) using an I^2C bus. The master microcontroller produces twelve pulse-width-modulation signals to control each servo separately. Each slave microcontroller reads and digitizes data from the force sensors and transmits it to the master microcontroller.

Stickybot's controller must consider limb coordination, which presents two different and sometimes contradictory goals: force balancing and leg phasing. In addition, certain stable limb combinations must be in contact with the climbing surface at all times (i.e., Stickybot must use either a diagonal trot or tripedal crawl). To achieve this, three separate control laws for four different stages of leg motion (stance, detachment, flight, attachment) are implemented.

1) Stance Controller: During stance, the controller implements force balancing using a grasp-space stiffness controller, similar to controllers used for dexterous manipulation (e.g. [7],[21]).

Since Stickybot uses servomotors that only accept position commands, the stiffness control law is given as:

$$\mathbf{x_{cmd}}(s) = \mathbf{x_{ff}}(s) + \left(k_P + \frac{k_I}{s}\right)\mathbf{C}\left(\mathbf{f_s}(s) - \mathbf{f_d}(s)\right) \quad (7)$$

where $\mathbf{x_{cmd}}$ is a vector comprised of the stroke servo commanded positions, $\mathbf{x_{ff}}$ is the feed forward position command, k_P and k_I are the proportional and integral gains respectively, $\mathbf{C}$ is the compliance matrix, $\mathbf{f_s}$ is a vector

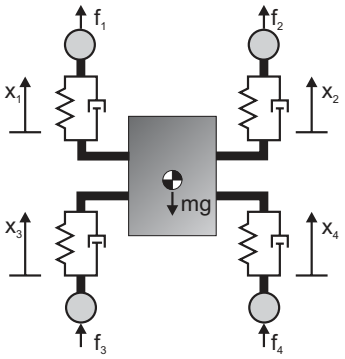

Fig. 9. Schematic used to generate values for the grasp matrix

comprised of sensed traction forces from each leg, and $\mathbf{f_d}$ is a vector of desired traction forces. A diagonal compliance matrix would result in independent leg control, which is useful during attachment and detachment; however, during stance we desire leg coupling and thus $\mathbf{C}$ is defined as:

$$\mathbf{C} = \mathbf{G}^{-1}\mathbf{C_0}\mathbf{G} \tag{8}$$

where $\mathbf{C_0}$ is a diagonal gain matrix chosen such that $\mathbf{C_0} \neq \mathbf{I}$ and $\mathbf{G}$ is the grasp matrix given as:

$$\mathbf{G} = \frac{1}{2}\begin{bmatrix} 1 & 1 & 1 & 1 \\ 1 & -1 & 1 & -1 \\ 1 & 1 & -1 & -1 \\ 1 & -1 & -1 & 1 \end{bmatrix} \tag{9}$$

The grasp matrix is comprised of four independent "grasp modes." The first row in $\mathbf{G}$ is formed by summing the grasp forces in the Y-direction (Fig. 9). The second row is produced by summing the moments about the center of mass. The third and fourth rows are chosen such that $\mathbf{G}$ is orthogonal. The chosen values correspond to a fore-aft coupling and a diagonal coupling of the legs respectively. The implementation of stiffness control in grasp space creates a framework for force distribution. By increasing the compliances of all but the total-traction mode, the robot will evenly distribute the forces between feet and achieve force balance while remaining stiff to other variations in loading.

2) Attachment and Detachment Controller: This controller is identical to the stance controller except that $\mathbf{C} = \mathbf{I}$, which allows each leg to act independently.

3) Flight Controller: During flight, the controller performs phase adjustments, which effectively keep the legs close to a predefined gait. The flight controller is inspired by [12] and defined as:

$$x_{cmd\_i}(s) = \frac{v_{ff}}{s} + k\left(\phi_i - \frac{\phi_{i+1} + \phi_{i-1}}{2}\right) \tag{10}$$

where v_{ff} is a feed forward velocity, k is a proportional gain, ϕ_i is the phase angle along a nominal leg trajectory, $\phi \in [0, 1]$, and i is the leg detachment order, $i = 1 \ldots 4$.

III. Results

Stickybot is capable of climbing a variety of surfaces at 90 deg including glass, glossy ceramic tile, acrylic, and polished granite at speeds up to 4.0 cm/s (0.12 body-lengths/s, excluding the tail). The maximum speed of Stickybot on level ground is 24cm/s and is limited by its actuators (Table I).

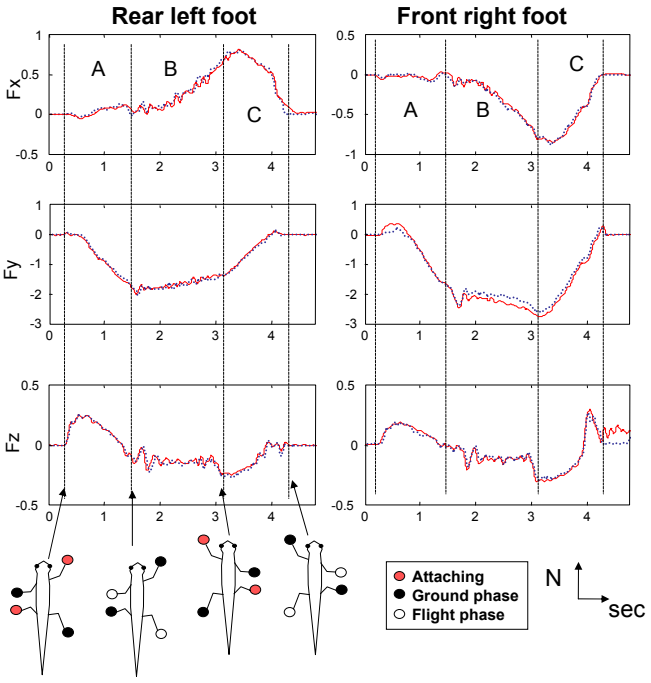

Fig. 10. Force plate data of rear left foot (left) and front right foot (right) of Stickybot climbing with a 6s period at a speed of 1.5 cm/s. Data filtered at 10Hz. Two successive runs are shown to illustrate repeatability.

Figure 10 presents force plate data of Stickybot climbing vertical glass. The left side shows data from the rear left foot and the right side displays data from the front right foot. Data from two successive runs are shown to give an indication of the typical repeatability.

Section A (0 to 1.5 s) represents the preloading and flexing of the foot. There is almost no force in the lateral (X) direction during preload and the traction force (-Y) is increasing. Although each foot would ideally engage with negligible normal force, there is a small amount of positive normal force during engagement. Weight transfer between diagonal pairs also occurs during section A.

Section B represents the ground stroke phase. There are equal and opposite forces in the X direction for the front right and rear left feet, indicating that the legs are pulling in toward the body. This helps stabilize the body and is similar to the lateral forces exhibited in geckos (and in contrast to the *outward* lateral forces observed in small lizards and insects) [3]. The Y-direction shows relatively steady traction force, and the Z-direction indicates adhesion on both the front and rear feet. Note that this differs from gecko data, in which the rear feet exhibit positive normal force [3]. This is due to the fact that Stickybot uses its tail to prevent the body from pitching back, whereas geckos use their rear feet.

In section C the feet release both by reducing the traction force (Y) and by peeling (utilizing digital hyperextension). Both front and rear feet exhibit low detachment forces in the Z-direction, especially the rear foot. Note also that the transition between B and C is accompanied by a temporary increase in adhesion (-Z force) and subsequently decreases

as the opposite diagonal feet engage.

TABLE I

PHYSICAL PARAMETERS FOR *Stickybot*

Body size	600 x 200 x 60 mm (excluding cables)
Body mass	370 g (including batteries and servo circuitry)
Maximum speed	4.0 cm/s (0.05 bodylength/s)
Servo motors	Hitec HB65 x 8 Hs81 x 4
Batteries	lithium polymer x2 (3.7 V, 480 mAh per pack)

IV. CONCLUSIONS AND FUTURE WORK

Taking cues from geckos, Stickybot uses three main principles to climb smooth surfaces. First, it employs *hierarchical compliance* that conforms at levels ranging from the micro- to centimeter scale. Second, Stickybot takes advantage of *directional adhesion* that allows it to smoothly engage and disengage from the surface by controlling the traction force. This prevents large disengagement forces from propagating throughout the body and allows the feet to adhere to surfaces when loaded in shear. Interestingly, the motion strategy for engaging adhesives is similar to that used for microspines [1]. Third, Stickybot employs *force control* that works in conjunction with the body compliance and adhesive directional patches to control the traction forces in the feet.

Several improvements to Stickybot are planned. The introduction of better adhesive structures with improved hierarchical compliance will allow Stickybot to climb rougher surfaces and yield longer climbs with increased dirt resistance. Another degree of freedom at the ankle joints is necessary to climb downward. Additional sensors in the feet will allow the robot to detect when proper contact has been made, which will improve the reliability of climbing on varying surfaces. Once the climbing technology is more mature, the ability to climb smooth surfaces will be integrated into the RiSE family of robots in an attempt to design a machine capable of climbing a wide variety of man-made and natural surfaces using a combination of adhesion and microspines [19].

ACKNOWLEDGEMENTS

We thank Jonathan Karpick, Sanjay Dastoor, and Arthur McClung for their help in circuit board fabrication, coding, and gait generation in support of Stickybot. The development of Stickybot is supported by the DARPA BioDynotics program. Matthew Spenko is supported by the Intelligence Community Postdoctoral Fellow Program.

REFERENCES

[1] A. Asbeck, S. Kim, M. Cutkosky, W. Provancher, and M. Lanzetta. Scaling hard vertical surfaces with compliant microspine arrays. *International Journal of Robotics Research*, 2006.

[2] K. Autumn, A. Dittmore, D. Santos, M. Spenko, and M. Cutkosky. Frictional adhesion: a new angle on gecko attachment. *J Exp Biol*, 209(18):3569–3579, 2006.

[3] K. Autumn, S. T. Hsieh, D. M. Dudek, J. Chen, C. Chitaphan, and R. J. Full. Dynamics of geckos running vertically. *J Exp Biol*, 209(2):260–272, 2006.

[4] K. Autumn, M. Sitti, Y. Liang, A. Peattie, W. Hansen, S. Sponberg, T. Kenny, R. Fearing, J. Israelachvili, and R. Full. Evidence for van der waals adhesion in gecko setae. *Proc. of the National Academy of Sciences of the USA*, 99(19):12252–12256, 2002.

[5] C. Balaguer, A. Gimenez, J. Pastor, V. Padron, and C. Abderrahim. A climbing autonomous robot for inspection applications in 3d complex environments. *Robotica*, 18(3):287–297, 2000.

[6] M. Binnard and M. Cutkosky. A design by composition approach for layered manufacturing. *ASME J Mechanical Design*, 122(1), 2000.

[7] M. Buss and K. P. Kleinmann. Multi-fingered grasping experiments using real-time grasping force optimization. In *ICRA*, volume 2, pages 1807–1812, 1996.

[8] K. Daltorio, S. Gorb, A. Peressadko, A. Horchler, R. Ritzmann, and R. Quinn. A robot that climbs walls using micro-structured polymer feet. In *CLAWAR*, 2005.

[9] K. Daltorio, A. Horchler, S. Gorb, R. Ritzmann, and R. Quinn. A small wall-walking robot with compliant, adhesive feet. In *International Conference on Intelligent Robots and Systems*, 2005.

[10] H. Gao, X. Wang, H. Yao, S. Gorb, and E. Arzt. Mechanics of hierarchical adhesion structures of geckos. *Mechanics of Materials*, 37:275–285, 2005.

[11] S. Gorb, M. Varenberg, A. Peressadko, and J. Tuma. Biomimetic mushroom-shaped fibrillar adhesive microstructure. *Journal of The Royal Society Interface*, 2006.

[12] G.C. Haynes and A. Rizzi. Gait regulation and feedback on a robotic climbing hexapod. In *Robotics: Science and Systems*, Philadelphia, 2006.

[13] K.L. Johnson, K. Kendall, and A.D. Roberts. Surface energy and the contact of elastic solids. *Proc. of the Royal Society A: Mathematical, Physical and Engineering Sciences*, 324(1558):301–313, 1971.

[14] S. Kim and M. Sitti. Biologically inspired polymer microfibers with spatulate tips as repeatable fibrillar adhesives. *Applied Physics Letters*, 89(261911), 2006.

[15] G. La Rosa, M. Messina, G. Muscato, and R. Sinatra. A lowcost lightweight climbing robot for the inspection of vertical surfaces. *Mechatronics*, 12(1):71–96, 2002.

[16] M. Northen and K. Turner. A batch fabricated biomimetic dry adhesive. *Nanotechnology*, 16:1159–1166, 2005.

[17] A. Peressadko and S.N. Gorb. When less is more: experimental evidence for tenacity enhancement by division of contact area. *Journal of Adhesion*, 80(4):247–261, 2004.

[18] D. Santos, S. Kim, M. Spenko, A. Parness, and M. Cutkosky. Directional adhesive structures for controlled climbing on smooth vertical surfaces. In *IEEE ICRA*, Rome, Italy, 2007. Accepted.

[19] A. Saunders, D. Goldman, R. Full, and M. Buehler. The rise climbing robot: body and leg design. In *SPIE Unmanned Systems Technology VII*, volume 6230, Orlando, FL, 2006.

[20] M. Sitti and R. Fearing. Synthetic gecko foot-hair micro/nano-structures as dry adhesives. *Adhesion Science and Technology*, 17(8):1055, 2003.

[21] J. Son and R. D. Howe. Performance limits and stiffness control of multifingered hands. In O. Khatib and J. K. Salisbury, editors, *Experimental Robotics IV*, volume 223 of *Lecture Notes in Control and Information Sciences*, pages 91–102. Springer-Verlag, 1997.

[22] O. Unver, M. Murphy, and M. Sitti. Geckobot and waalbot: Small-scale wall climbing robots. In *AIAA 5th Aviation, Technology, Integration, and Operations Conference*, 2005.

[23] O. Unver, A. Uneri, A. Aydemir, and M. Sitti. Geckobot: a gecko inspired climbing robot using elastomer adhesives. In *IEEE ICRA*, pages 2329–2335, Orlando, FL, 2006.

[24] vortex. www.vortexhc.com, 2006.

[25] L. E. Weiss, R. Merz, F. Prinz, G. Neplotnik, P. Padmanabhan, L. Schultz, and K. Ramaswami. Shape deposition manufacturing of heterogenous structures. *Journal of Manufacturing Systems*, 16(4):239–248, 1997.

[26] Z. Xu and P. Ma. A wall-climbing robot for labeling scale of oil tank's volume. *Robotica*, 20(2):203–207, 2002.

[27] H. Yoshizawa, Y. Chen, and J. Israelachvili. Fundamental mechanisms of interfacial friction. 1. relation between adhesion and friction. *Journal of Physical Chemistry*, 97:4128–4140, 1993.

[28] Y. Zhao, T. Tong, L. Delzeit, A. Kashani, M. Meyyapan, and A. Majumdar. Interfacial energy and strength of multiwalled-carbon-nanotube-based dry adhesive. *Vacuum Science and Tech B*, 2006.

[29] J. Zhu, D. Sun, and S.K. Tso. Development of a tracked climbing robot. *Intelligent and Robotic Systems*, 35(4):427–444, 2002.